Aerosol and Air Quality Research, 17: 1073–1083, 2017

ISSN: 1680-8584 print / 2071-1409 online
doi: 10.4209/aaqr.2016.07.0322

Direct Simulation Monte Carlo Method for Acoustic Agglomeration under Standing Wave Condition

Fengxian Fan[1,2*], Mingjun Zhang[1,2], Zhengbiao Peng[3], Jun Chen[1,2], Mingxu Su[1,2], Behdad Moghtaderi[3], Elham Doroodchi[3]

[1] *School of Energy and Power Engineering, University of Shanghai for Science and Technology, Shanghai 200093, China*
[2] *Shanghai Key Laboratory of Multiphase Flow and Heat Transfer in Power Engineering, University of Shanghai for Science and Technology, Shanghai 200093, China*
[3] *Discipline of Chemical Engineering, School of Engineering, The University of Newcastle, NSW 2308, Australia*

ABSTRACT

Acoustic agglomeration proves promising for preconditioning fine particles (i.e., $PM_{2.5}$) as it significantly improves the efficiency of conventional particulate removal devices. However, a good understanding of the mechanisms underlying the acoustic agglomeration in the standing wave is largely lacking. In this study, a model that accounts for all of the important particle interactions, e.g., orthokinetic interaction, gravity sedimentation, Brownian diffusion, mutual radiation pressure effect and acoustic wake effect, is developed to investigate the acoustic agglomeration dynamics of $PM_{2.5}$ in the standing wave based on the framework of direct simulation Monte Carlo (DSMC) method. The results show that the combination of orthokinetic interaction and gravity sedimentation dominates the acoustic agglomeration process. Compared with Brownian diffusion and the mutual radiation pressure effect, the acoustic wake plays a relatively more important role in governing the particle agglomeration. The phenomenon of particle agglomeration becomes more pronounced when the acoustic frequency and intensity are increased. The model is shown to be capable of accurately predicting the dynamic acoustic agglomeration process in terms of the detailed evolution of particle size and spatial distribution, which in turn allows for the visualization of important features such as "orthokinetic drift". The prediction results are in good agreement with the experimental data.

Keywords: Fine particles ($PM_{2.5}$); Acoustic agglomeration; Standing wave; Direct simulation Monte Carlo (DSMC) method; Numerical simulation.

INTRODUCTION

Particles with an aerodynamic diameter not greater than 2.5 μm are referred to as fine particles, or $PM_{2.5}$. These particles are generated mainly from coal-fired power plants, industrial processes and vehicles (Ehrlich *et al.*, 2007; Li *et al.*, 2013; Pui *et al.*, 2014). Due to the small particle size, it is extremely difficult for the conventional devices, e.g., bag filters, electrostatic precipitators (ESPs), cyclones and wet scrubbers, to effectively remove $PM_{2.5}$ from the flue gas. Consequently, a large amount of $PM_{2.5}$ is emitted into the atmosphere, causing a board range of adverse effects to human health. It has been reported that the collection efficiency of $PM_{2.5}$ using conventional devices can be improved by means of preconditioning technologies such as acoustic agglomeration (Hoffmann, 2000; Liu *et al.*, 2009; Fan *et al.*, 2013), electric agglomeration (Chang *et al.*, 2015) and heterogeneous condensation (Fan *et al.*, 2009; Yang *et al.*, 2010). Amongst these technologies, acoustic agglomeration that applies an intense acoustic field to manipulate the motion, collision and hence agglomeration of $PM_{2.5}$, has been recognized as a promising method for the removal of $PM_{2.5}$. Under the acoustic field, the fine particles coagulate into large agglomerates which can then be collected using the conventional devices.

Experiments have been carried out in the past decades to determine the factors affecting the agglomeration behavior of $PM_{2.5}$ under the acoustic field (Volk *et al.*, 1976; Rajendran *et al.*, 1979; Tiwary *et al.*, 1984; Hoffmann *et al.*, 1993; Kashkoush and Busnaina, 1993; Sharifi *et al.*, 1994; Capéran *et al.*, 1995; Manoucheri and Ezekoye, 1996; Gallego-Juárez *et al.*, 1999; Spengler and Jekel, 2000; De Sarabia *et al.*, 2003; Komarov *et al.*, 2004; Liu *et al.*, 2009; Liu *et al.*, 2011; Wang *et al.*, 2011; Yan *et al.*, 2015). The experimental results indicated that the removal efficiency using acoustic agglomeration depends on the acoustic frequency and

* Corresponding author.
Tel.: 86-21-55271751; Fax: 86-21-55272376
E-mail address: fanfengxian@hotmail.com

intensity, particle size and concentration, and residence time. However, a good understanding of the mechanisms underlying the acoustic agglomeration is still largely lacking. Attempts through theoretical analysis have also been directed towards the explanation of the occurrence of the acoustic agglomeration phenomenon (Shaw and Tu, 1979; Chou and Shaw, 1981; Chou *et al.*, 1982). Different mechanisms of acoustic agglomeration, e.g., orthokinetic and hydrodynamic interactions and acoustically induced turbulent deposition, have been reported. The orthokinetic interaction is described as the relative motion of particles induced by the viscous entrainment of the acoustic wave. The acoustic particle entrainment associated with orthokinetic interaction has been reported in many studies (e.g., Hoffmann and Koopmann, 1996; Hoffmann and Koopmann, 1997; González *et al.*, 2000; Cleckler *et al.*, 2012). The hydrodynamic interaction consists of the mutual radiation pressure effect that represents Bernoulli's hydrodynamic principle and the acoustic wake effect caused by asymmetric flow fields around the particles under the Oseen flow condition (Hoffmann and Koopmann, 1996). The particle interactions due to the mutual radiation pressure effect and the acoustic wake effect have been observed in both experiments and model simulations (Hoffmann and Koopmann, 1996; Hoffmann and Koopmann, 1997; González *et al.*, 2001; González *et al.*, 2002; González *et al.*, 2003). Generally, the acoustic turbulence occurs at an acoustic intensity higher than 160 dB (Chou *et al.*, 1982; Tiwary *et al.*, 1984; Chen *et al.*, 2008). Therefore, for an acoustic intensity less than 160 dB, the acoustic particle interactions are mainly caused by the orthokinetic interaction, the mutual radiation pressure effect and the acoustic wake effect.

As the computer technologies advance, investigations of acoustic agglomeration using numerical models become increasingly popular. Three numerical simulation methods, namely sectional method (Ezekoye and Wibowo, 1999; Zhang *et al.*, 2012), method of moment (Zhang *et al.*, 2011) and direct simulation Monte Carlo (DSMC) method (Funcke and Frohn, 1995; Sheng and Shen, 2006; Sheng and Shen, 2007) have been generally employed in the literature for predicting the particle agglomeration. However, the DSMC method has shown great advantages over the other two methods (Zhang and Fan, 2012; Wei, 2013). The sectional method and the method of moment solve mathematical equations for particle agglomeration through an appropriate discretization scheme or by quadrature. The numerical implementation of these methods is complicated, causing difficulties in programing. Moreover, discrete errors using these methods are generally large. The DSMC method describes directly the dynamic evolution of particle position, size and number in a dispersed system through an amount of random samples from the system. The DSMC method itself has discrete nature, making it easier to program and better to reflect the physical process compared with the former methods. Furthermore, in the DSMC method, the real particles are replaced by the sample particles, leading to a much less number of particles to be simulated and hence a substantial reduction in the computational time. Previous studies using the DSMC method for acoustic agglomeration have shed some insight into the role of orthokinetic interaction in the standing wave (Funcke and Frohn, 1995) and the roles of orthokinetic interaction and mutual radiation pressure effect in the travelling wave (Sheng and Shen, 2006; Sheng and Shen, 2007). However, questions remain as to whether the acoustic wake effect should be included or not. As the standing wave is much more efficient than the travelling wave (Rajendran *et al.*, 1979; Fan, 2008), it is necessary to develop an adaptable method by which our understanding of acoustic agglomeration, particularly in the standing wave, can be further improved. Sheng and Shen (2006, 2007) combined the DSMC model with the general dynamic equation for particle coagulation (Friedlander, 1997). Unfortunately, their method was unable to track the particle trajectories and accordingly failed to capture the evolution of the spatial distribution of particles. Recently, the DSMC method has been adopted by our group to investigate the particle collision rate due to the orthokinetic interaction in the standing wave (Fan *et al.*, 2013). The trajectories of sample particles have been tracked and the detailed dynamic process of acoustic collision has been demonstrated.

In the present work, the DSMC method is extended to study the acoustic agglomeration dynamics with the inclusion of the mutual radiation pressure effect and the acoustic wake effect. Benchmarked experimental data is used to validate the model developed in this study. The model is then applied to further investigate the phenomenon of acoustic agglomeration under the standing wave conditions. Specifically, the relevant importance of different mechanisms in governing the process of acoustic agglomeration has been discussed. Moreover, the effects of key operating conditions (i.e., acoustic frequency, acoustic intensity and initial particle size distribution) on the acoustic agglomeration have been investigated. The objective is to achieve a fundamental understanding of the mechanisms and physics underlying the phenomenon of acoustic agglomeration.

MODEL AND METHOD

The acoustic agglomeration occurring in a chamber is considered. The standing wave is generated by the superposition of a sinusoidal incident wave propagating along the horizontal direction and its own reflected wave. For clarity, let's take the direction of the wave motion as x, the gravitational direction as z, and the direction perpendicular to x and z as y. Prior to the application of the acoustic field, the particles are carried along by the gas flow in the y direction.

Equations of Wave Motion

The equation of wave motion for the standing wave in the non-rotational and inviscid gas can be derived as (Bruneau, 2006)

$$u_{gx}(x, t) = u_a \sin(kx) \sin(2\pi ft) \quad (1)$$

where $u_{gx}(x,t)$ is the oscillating velocity of the gas at position x and time t; u_a is the velocity amplitude; k is the wave

number; and f is the frequency.

The viscosity and rotation of the flow field around a particle can be neglected, if the following relations are satisfied (Cleckler *et al.*, 2012)

$$d_p/\lambda << 1 \tag{2}$$

$$d_p^2 c\rho_g/(\mu_g\lambda) << 1 \tag{3}$$

$$\mathrm{Re}_p = \rho_g \left|\vec{u}_g - \vec{u}_p\right| d_p / \mu_g << 1 \tag{4}$$

where d_p is the particle diameter; λ is the wavelength; Re_p is the particle Reynold number; ρ_g is the gas density; $\vec{u}_g$ and $\vec{u}_p$ are the gas and particle velocities, respectively; μ_g is the dynamic viscosity of the gas; and c is the speed of sound. While it can be easily obtained that relations (2) and (3) are well satisfied, the particle velocity needed to compute Re_p is not directly available. However, Re_p can be estimated using $\mathrm{Re}_p \approx \rho_g|u_{gx} - u_{px}|d_p/\mu_g \le \rho_g u_a(1-\eta)d_p/\mu_g$, where η is the particle entrainment coefficient represented in a function of the acoustic frequency and the particle relaxation time (Hoffmann and Koopmann, 1996; González *et al.*, 2000). For the $PM_{2.5}$ subjected to the acoustic field presented in this work, $\mathrm{Re}_p \le 0.13$ is obtained. Therefore, Eq. (1) can be used as an approximate solution to describe the gas velocity induced by the acoustic wave.

The acoustic intensity described by the sound pressure level, L (dB), is often used to describe the acoustic field. It can be expressed as a function of the gas velocity amplitude

$$L = 20\log_{10}\left(\frac{u_a c\rho_g}{\sqrt{2}P_r}\right) \tag{5}$$

where P_r is the reference sound pressure, and $P_r = 2 \times 10^{-5}$ Pa.

Equations of Particle Motion

Forces acting on a particle in the acoustic field include the gravitational force, the buoyancy force, the drag force, and the unsteady forces (e.g., the Basset force, the virtual mass force and the pressure gradient force). Since pervious work has shown that the unsteady forces are negligible compared with the drag force (Cleckler *et al.*, 2012), the equations of particle motion can be written as

$$m_p \frac{\mathrm{d}u_{px}}{\mathrm{d}t} = 3\pi\mu_g d_p (u_{gx} - u_{px})/C_c \tag{6a}$$

$$m_p \frac{\mathrm{d}u_{py}}{\mathrm{d}t} = 3\pi\mu_g d_p (u_{gy} - u_{py})/C_c \tag{6b}$$

$$m_p \frac{\mathrm{d}u_{pz}}{\mathrm{d}t} = -3\pi\mu_g d_p u_{pz}/C_c + \frac{1}{6}(\rho_p - \rho_g)\pi d_p^3 g \tag{6c}$$

where m_p is the particle mass; ρ_p is the particle density; g is the acceleration of gravity; and the subscripts x, y and z represent the components along the x, y and z directions, respectively. C_c is the Cunningham slip correction coefficient, given by

$$C_c = 1 + \mathrm{Kn}[1.257 + 0.400\exp(-1.100/\mathrm{Kn})] \tag{7}$$

where Kn is the Knudsen number, which is defined as $\mathrm{Kn} = 2\lambda_g/d_p$ with λ_g being the mean free path of gas molecules.

Note that the first terms on the RHS of Eqs. (6) are the components of the drag force in the Stokes flow regime ($\mathrm{Re}_p << 1$). For increasing Re_p, the Stokes drag force (F_s) can be extended to Oseen drag force (F_o) to include the first-order inertial effect in the form of $F_o = F_s(1 + 3\mathrm{Re}_p/16)$ (Dianov *et al.*, 1968; González *et al.*, 2001).

The particle velocity can be solved by Eqs. (6). Subsequently, the particle displacement is calculated by

$$\vec{S}_p(t+\Delta t) = \vec{S}_p(t) + \frac{\Delta t}{2}\left[\vec{u}_p(t+\Delta t) + \vec{u}_p(t)\right] \tag{8}$$

where $\vec{S}_p(t+\Delta t)$ is the particle displacement at time $t + \Delta t$. Δt is the time step and often substantially smaller than both the sound period $1/f$ and the particle relaxation time τ to achieve the high computational accuracy,

$$\Delta t << 1/f \tag{9}$$

$$\Delta t << \tau = \frac{\rho_p d_p^2 C_c}{18\mu_g} \tag{10}$$

DSMC Method

DSMC method is employed to predict the particle collision and the subsequent agglomeration behavior. The computational domain is divided into a number of small cells. It is assumed that the collision is binary and occurs only between particles residing in the same cell. The probability of particle i colliding with other particles in the time interval $\Delta t'$ is expressed as

$$P_i = \sum_{j=1}^{N} P_{ij} = \sum_{j=1}^{N} \beta_{ij} w_j \Delta t'/V_{ci} \tag{11}$$

where P_i is the collision probability between sample particle i and all other particles; P_{ij} is the collision probability between particle i and j; N is the number of the sample particles within the cell of particle i; β_{ij} is the collision rate between particle i and j; w_j is the number weight of the sample particle j (i.e., the number of real particles the sample particle j represents); and V_{ci} is the volume of the cell in which particle i resides.

The collision rate (also called the agglomeration kernel) β_{ij} is used to represent the effect of particle interactions on the acoustic agglomeration. Besides the acoustically induced particle interactions, Brownian diffusion as a result of the particles' random motions and gravity sedimentation due to the difference in the particle settling velocities can, in principle, induce particle agglomeration. Therefore, all of

the important particle interaction mechanisms including the Brownian diffusion, the gravity sedimentation, the orthokinetic interaction, the mutual radiation pressure effect and the acoustic wake effect are considered in the present work. The overall collision rate β_{ij} can be obtained from the mechanisms mentioned above using a simple additive method

$$\beta_{ij} = \beta_{ij}^{Bro} + \beta_{ij}^{Gra} + \beta_{ij}^{Orth} + \beta_{ij}^{MRP} + \beta_{ij}^{AW} \tag{12}$$

where β_{ij}^{Bro}, β_{ij}^{Gra}, β_{ij}^{Orth}, β_{ij}^{MRP} and β_{ij}^{AW} are the collision rates due to the Brownian diffusion, the gravity sedimentation, the orthokinetic interaction, the mutual radiation pressure effect and the acoustic wake effect, respectively.

The combined effect of the orthokinetic interaction and the gravity sedimentation can be obtained from the relative motion of particle i and j based on the numerical solutions of Eqs. (6)

$$\beta_{ij}^{Orth} + \beta_{ij}^{Gra} = \frac{\pi}{4}(d_{pi} + d_{pj})^2 \left|\vec{u}_{pij}\right| \tag{13}$$

where $\vec{u}_{pij}$ is the relative velocity between particle i and j.

When submicron- or micron-sized particles are considered, agglomeration caused by Brownian diffusion may be significant. The collision rate between particle i and j due to Brownian diffusion is given by (Sheng and Shen, 2006)

$$\beta_{ij}^{Bro} = \frac{2k_B T}{3\mu_g}(d_{pi} + d_{pj})(C_{ci}/d_{pi} + C_{cj}/d_{pj}) \tag{14}$$

where k_B is the Boltzmann constant; and T is the temperature.

The collision rate resulting from the mutual radiation pressure effect and the acoustic wake effect in the travelling wave have been derived by Song (1990) and Dong *et al.* (2006). Here, the collision rate is extended to suit the standing wave condition using the local velocity amplitude

$$\beta_{ij}^{MRP} = \frac{\sqrt{3}\rho_g u_a^{\,2}\sin^2(kx)}{144\pi\mu_g}\frac{d_{pi}^{\,2} d_{pj}^{\,2}}{d_{pi} + d_{pj}} g_{ij}(r) \tag{15}$$

$$\beta_{ij}^{AW} = \frac{3}{16}\frac{u_a \sin(kx)}{r}(d_{pi} + d_{pj})^2 (d_{pi} l_i + d_{pj} l_j) \tag{16}$$

where $g_{ij}(r)$ is the hydrodynamic interaction function based on the mutual radiation pressure effect, which is a function of the separation distance between the particles, r. $g_{ij}(r)$ depends also on the longitudinal wave strength parameter, the viscous wave strength parameter, the longitudinal wavenumber, and the viscous wavenumber. For details of $g_{ij}(r)$ see (Song, 1990). Moreover, l is the slip coefficient and reads

$$l_i = \frac{l_{si}}{1 + h_i l_{si}^2} \tag{17}$$

$$l_{si} = \frac{2\pi f \tau_i}{\sqrt{1 + (2\pi f \tau_i)^2}} \tag{18}$$

$$h_i = \frac{9u_a \sin(kx)}{2\pi^2 f d_{pi}}\frac{\rho_g}{\rho_p} \tag{19}$$

To include all collision events, the time interval $\Delta t'$ must be sufficiently small to ensure $P_i < 1$ for each sample particle. According to Eq. (11), the time interval satisfies

$$\Delta t' < 1 \Big/ \max_{\forall i}\left[\sum_{j=1}^{N}(\beta_{ij}\omega_j / V_{ci})\right] \tag{20}$$

The modified Nanbu method (Tsuji *et al.*, 1998) is used to judge the occurrence of collision between a pair of sample particles. A random number R with a uniform distribution in the interval [0, 1) is generated. Subsequently, a candidate collision partner of sample particle i (i.e., the sample particle j) is selected from the sample particles in the same cell following

$$j = \text{int}[R \times N] + 1 \tag{21}$$

where int[$R \times N$] represents the integer part of $R \times N$.

It is considered that the sample particle i collides with the selected sample particle j during the time interval $\Delta t'$ if

$$R > \frac{j}{N} - P_{ij} \tag{22}$$

It is assumed that all of the collisions lead to agglomeration. To reflect the consequence of the agglomeration event, the number weight, the volume and the velocity of the colliding sample particles are adjusted (Zhao *et al.*, 2005).

The velocity of the formed agglomerate $\vec{u}_{agg}$ is given by the conservation of momentum

$$\vec{u}_{agg} = \frac{m_{pi}\vec{u}_{pi}^{\,0} + m_{pj}\vec{u}_{pj}^{\,0}}{m_{pi} + m_{pj}} \tag{23}$$

where superscript 0 indicates the value just before the collision.

The post-collisional number weight, volume, and velocity of the colliding sample particles are updated by (Zhao *et al.*, 2005; Zhang and Fan, 2012):

If $w_i = w_j$,

$$w_i^{new} = w_i / 2, \quad V_i^{new} = V_i^0 + V_j^0, \quad \vec{u}_{pi}^{\,new} = \vec{u}_{agg} \tag{24a}$$

$$w_j^{new} = w_j / 2, \quad V_j^{new} = V_i^0 + V_j^0, \quad \vec{u}_{pj}^{\,new} = \vec{u}_{agg} \tag{24b}$$

If $w_i > w_j$,

$$w_i^{new} = w_i - w_j, \quad V_i^{new} = V_i^0, \quad \vec{u}_{pi}^{new} = \vec{u}_{pi}^0 \tag{25a}$$

$$w_j^{new} = w_j, \quad V_j^{new} = V_i^0 + V_j^0, \quad \vec{u}_{pj}^{new} = \vec{u}_{agg} \tag{25b}$$

If $w_i < w_j$,

$$w_i^{new} = w_i, \quad V_i^{new} = V_i^0 + V_j^0, \quad \vec{u}_{pi}^{new} = \vec{u}_{agg} \tag{26a}$$

$$w_j^{new} = w_j - w_i, \quad V_j^{new} = V_j^0, \quad \vec{u}_{pj}^{new} = \vec{u}_{pj}^0 \tag{26b}$$

where superscript *new* indicates the post-collisional value.

Simulation Procedure

A three-dimensional domain with a volume of $\lambda \times 10$ mm $\times$ 10 mm is considered. The domain is evenly divided into 100 cells along the x direction. Initially, the sample particles with a number weight w_0 are uniformly distributed in the domain. The initial average velocity components of the sample particles in x, y and z directions are 0, 0.5 m s^{-1} and 0, respectively, and each velocity component has a random fluctuation in the range from –0.02 m s^{-1} to 0.02 m s^{-1}. Based on Eqs. (9), (10) and (20), the time step Δt for solving the particle motion and the time interval $\Delta t'$ for calculating the particle collision can be estimated. The computational parameters used in the simulations are listed in Table 1.

Steps of the numerical simulation are detailed as follows:

(1) The gas flow field and the particle distribution are initialized. Sample particles are generated according to the initial particle size distribution. Meanwhile, the number weight, the velocity and the position of the sample particles are specified.
(2) New velocities and positions of all the sample particles after the time step Δt are calculated using the equations of particle motion (i.e., Eqs. (6) and (8)).
(3) The locations of the particles are updated. For particles not in the simulation domain, the periodic boundary condition is applied to relocate the particles.
(4) Steps (2) and (3) are repeated for $\Delta t/\Delta t'$ times.
(5) The collision pairs are searched using the DSMC method. If two particles collide with each other, the agglomeration events are handled by changing the number weight, volume, and velocity according to Eqs. (24)–(26).
(6) Steps (2)–(5) are repeated until the time reaches a specified value.

The numerical simulations are performed on a computer equipped with 4 CPUs (Intel i5) and RAM of 8192 MB. It takes 4–8 days to run a simulation case, depending on the number of computational particles, which ranges from 7650 to 30600.

RESULTS AND DISCUSSION

Model Validation

The experimental data on acoustic agglomeration of coal-fired $PM_{2.5}$ by Zhao (2007) is used to validate the model. For consistency, the acoustic wave used in the simulation is kept exactly the same as that used in the experiment (i.e., a standing wave with f = 1000 Hz and L = 158.5 dB). The prediction results with the Stokes drag force as well as the Oseen drag force and the experimental data of the particle size distribution at t = 3.2 s are shown in Fig. 1. It can be seen that the difference between the particle size distributions after acoustic agglomeration predicted with the two drag forces is negligibly small, because Re_p is not big enough to produce obvious differences in the drag

Table 1. Computational parameters used in the simulation.

Parameter	u_{gv}/(m s^{-1})	p_0/Pa	T/K	ρ_p/(kg m^{-3})	w_0	Δt/s	$\Delta t'$/s
Value	0.5	101325	300	2400	5000	8×10^{-8}	8×10^{-6}

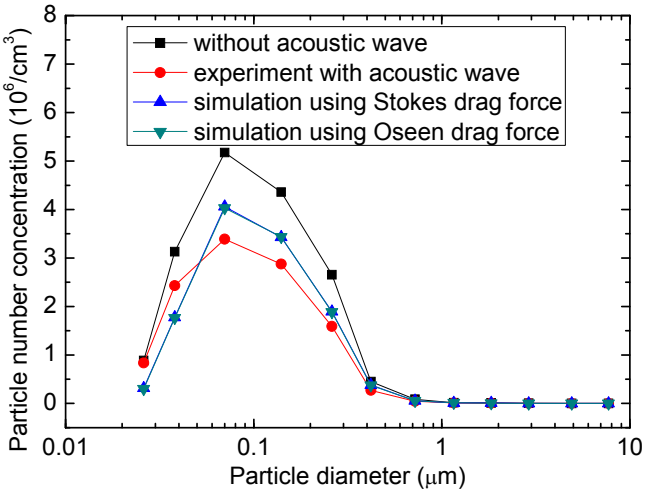

Fig. 1. Comparison with experiment of Zhao (2007). L = 158.5 dB, f = 1000 Hz, t = 3.2 s.

forces and in the consequent agglomeration rates. It can be also seen that the prediction results agree reasonably with the experimental data. Both the prediction results and the experimental data show that the particle number concentration decreases under the standing wave. The area under the particle size distribution curve obtained in the experiments is slightly smaller than that in the simulation, implying particles agglomerate to a greater extent in the experiments. This can be understood by the fact that the particles are assumed to be spheres in the simulation. In reality, the aggregates generated during the acoustic agglomeration of solid particles cannot be spherical. Instead, chain-like structures (Hoffmann and Koopmann, 1996; Komarov *et al.*, 2004; Liu *et al.*, 2009) are often observed. Compared with the equivalent spherical particle, the chain-like aggregate can be entrained more easily by the acoustic wave (Yang and Fan, 2015). Accordingly, the volume the aggregate sweeps during its oscillating motion is larger. Therefore, the particle interactions involving the aggregates could be underestimated if the aggregates are considered spherical.

Comparison of Different Agglomeration Mechanisms

Particle agglomeration in the acoustic field is governed by several mechanisms including the orthokinetic interaction, the gravity sedimentation, the Brownian diffusion, the mutual radiation pressure effect and the acoustic wake effect. The effect of the orthokinetic interaction on the acoustic agglomeration has been studied under both the travelling wave (Ezekoye and Wibowo, 1999; De Sarabia *et al.*, 2003; Sheng and Shen, 2006; Sheng and Shen, 2007; Zhang *et al.*, 2011; Zhang *et al.*, 2012) and the standing wave (Funcke and Frohn, 1995) conditions. The mutual radiation pressure effect under the travelling wave condition has also been reported in previous work (Ezekoye and Wibowo, 1999; Sheng and Shen, 2006; Sheng and Shen, 2007). However, investigation on acoustic agglomeration due to the mechanisms other than the orthokinetic interaction under the standing wave condition is very scarce. Therefore, it is necessary to examine the effect of the hydrodynamic particle interactions, specifically the mutual radiation pressure effect and the acoustic wake effect, on the acoustic agglomeration dynamics.

The simulation results of the acoustic agglomeration under different particle interaction mechanisms are given in Fig. 2. The particle size distribution before and after acoustic agglomeration is shown in Fig. 2(a) and the evolution of particle number concentration during acoustic agglomeration is shown in Fig. 2(b). The acoustic intensity and the frequency used in the simulations are 155 dB and 5000 Hz, respectively, and the residence time is 3 s. From Fig. 2(a) it can be seen that the particle number concentration in the submicron size range decreases remarkably and that in the micron size range increases slightly, indicating the occurrence of particle agglomeration. It is also noted that the particle number concentration in the micron size range is slightly higher when all of the particle interaction mechanisms are included than that obtained when only the orthokinetic interaction and the gravity sedimentation are considered. This suggests that other mechanisms apart from the orthokinetic interaction and the gravity sedimentation that drive acoustic agglomeration exist. Fig. 2(b) clearly demonstrates the effect of different mechanisms on the acoustic agglomeration. The combined effect of the orthokinetic interaction and the gravity sedimentation plays a dominant role in the particle agglomeration, whilst Brownian diffusion is negligible. With respect to the hydrodynamic interactions, the acoustic wake effect is more influential on the particle agglomeration behavior than the mutual radiation pressure effect. The result simply suggests that the acoustic wake effect should be taken into account in the numerical simulation or theoretical analysis of the acoustic agglomeration phenomenon.

Dynamic Process of Acoustic Agglomeration

Fig. 3 shows a sequence of snapshots during the acoustic agglomeration. It can be seen that an increasing number of particles drift to and gather at the wave node with the increase in the residence time. The drift motion of a single $PM_{2.5}$ under the standing wave has been theoretically described by Czyz (1987, 1990) and numerically analyzed

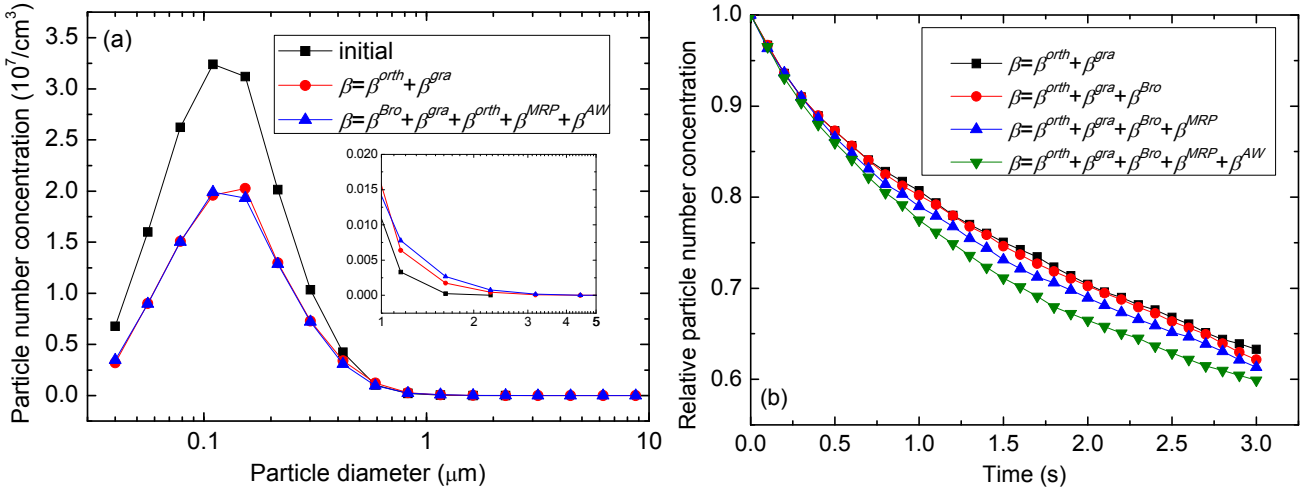

Fig. 2. Comparison of the effects of agglomeration mechanisms. L = 155 dB, f = 5000 Hz, t = 3 s. (a) Particle size distribution before and after acoustic agglomeration. (b) Evolution of total particle number concentration with time

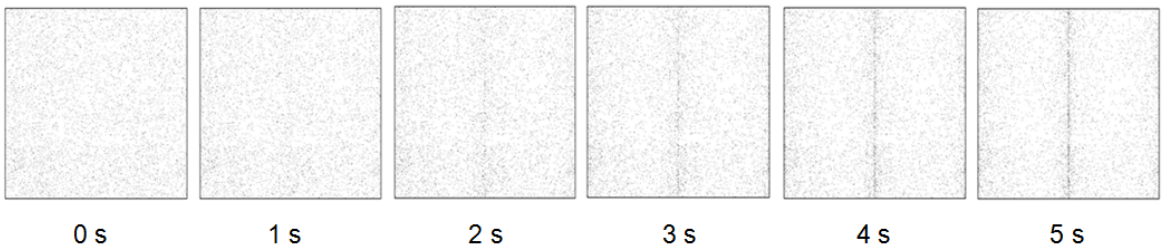

Fig. 3. Evolution of particle spatial distribution with time. L = 155 dB, f = 5000 Hz.

by Song and Fan (2016). It has been recognized that the particles with diameters above 0.5 μm are more prone to drift. The drift velocity decreases rapidly with the decrease in particle diameter when the diameter is less than 0.5 μm. The drift-to-node phenomenon results from the asymmetric motion of the gas in the standing wave. The drift velocity varies with the particle position and size (Song and Fan, 2016), thus the relative drift velocity may contribute to particle interaction and agglomeration. It is worth noting that the effect of the acoustic particle drift has not been modeled in previous simulations of acoustic agglomeration. Nevertheless, this effect is naturally included in the model developed in the present work in the equations of particle motion and in the collision rate of orthokinetic interaction. To distinguish the contributions of relative drift motion and oscillatory motion between the particles to the acoustic agglomeration, the former is henceforth referred to as "orthokinetic drift" and the later "orthokinetic oscillation". On this basis, the orthokinetic interaction involved in acoustic agglomeration under the standing wave condition is actually comprised of orthokinetic drift and orthokinetic oscillation. In addition to the orthokinetic drift, the drift-to-node motion of particles also leads to an increase of the local particle number concentration at the node, which in turn may contribute to the particle agglomeration. In our model, the effect of increased particle number concentration on the acoustic agglomeration is directly taken into account in the collision probability, since a higher particle number concentration leads to a greater collision probability as given by Eq. (11).

The evolutions of the particle size distribution and total particle number concentration are shown in Fig. 4. It can be seen that the concentration of small particles decreases and the concentration of large particles increases with time due to the formation of agglomerates by acoustic agglomeration. It is also found that total particle number concentration decreases monotonically with time but slowly for a long time, which is in accordance with the experimental findings (Manoucheri and Ezekoye, 1996; Liu *et al.*, 2009). The results indicate that the present model is capable of accurately capturing the phenomenon of acoustic agglomeration.

Effect of Acoustic Frequency

Fig. 5 shows the effect of acoustic frequency on the particle agglomeration. The acoustic intensity is constant at 155 dB and the residence time is 3 s. It is clearly shown that as the acoustic frequency increases, the particle number concentration peak decreases and the particle number concentration above 1 μm increases. This result is contrary to common beliefs that the acoustic agglomeration should be suppressed with increasing acoustic frequency, as the particle oscillatory motion is damped at a higher acoustic frequency. It is evident that the particle agglomeration becomes more pronounced at a higher acoustic frequency. For instance, the total particle number concentrations are reduced to 72.5%, 61.3% and 49.4% of the initial concentration after acoustic agglomeration at the frequency of 2000 Hz, 5000 Hz and 8000 Hz, respectively. This can be explained by the orthokinetic drift (i.e., the drift-to-node motion of the particles) in a standing wave. On the one hand, for the acoustic frequency range used here, the drift velocity increases with the increase of the frequency (Czyz, 1987, 1990; Song and Fan, 2016). On the other hand, increasing frequency shortens the wavelength. As a result, particles accumulate more rapidly, leading to more concentrated regions in the volume, which in turn induces more intense particle interactions and agglomeration due to the orthokinetic effect, the acoustic wake effect as well as the mutual radiation pressure effect. It is also worth noting that the effect of the acoustic frequency is not robust, instead it strongly depends on the particle size distribution (Gallego-Juárez *et al.*, 1999; Liu, *et al.*, 2011). Therefore, numerical and experimental investigations are still required to explore the effects of frequency on the acoustic agglomeration for different particle size distributions.

Effect of Acoustic Intensity

Fig. 6 gives the effect of acoustic intensity on the acoustic agglomeration at f = 5000 Hz and t = 3 s. As expected, both the peak of the particle size distribution and the total particle number concentration decrease when the acoustic intensity increases. Specifically, when the acoustic intensities are 145 dB, 150 dB and 155 dB, the total particle number concentrations decrease by 20.6%, 30.9%, and 38.7%, respectively. This is justifiable as the higher acoustic intensity produces the larger amplitude of particle oscillatory motion and the greater velocity of the particle drift-to-node motion, providing more opportunities for particles to collide due to the orthokinetic interaction. Meanwhile, faster drift-to-node motion leads to smaller separations between the particles, resulting in higher collision probability caused by both the acoustic wake effect and the mutual radiation pressure effect. The simulation results are well supported by previous experimental results which show that particle agglomeration is enhanced as the acoustic intensity increases (Gallego-Juárez *et al.*, 1999; Komarov *et al.*, 2004; Liu *et al.*, 2009; Yan *et al.*, 2015).

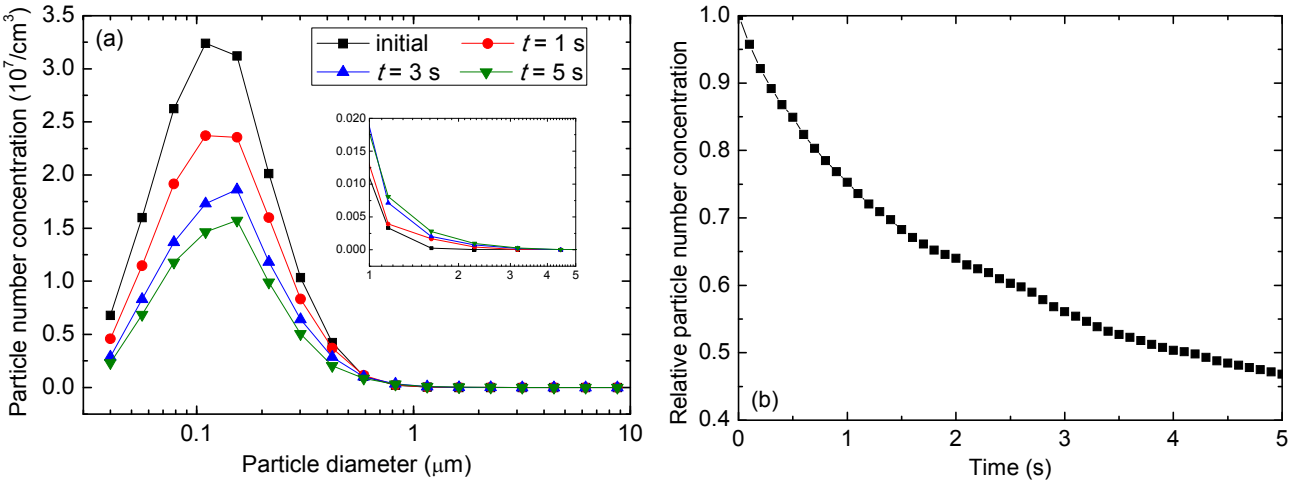

Fig. 4. Evolution of particle size and concentration with time. L = 155 dB, f = 5000 Hz. (a) Evolution of particle size distribution with time. (b) Evolution of total particle number concentration with time.

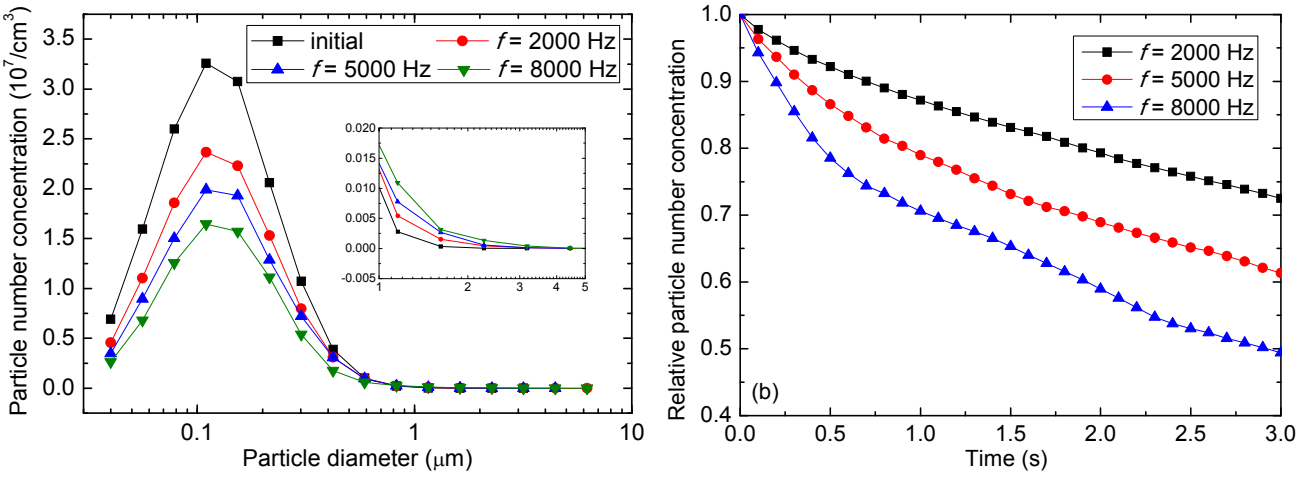

Fig. 5. Effect of acoustic frequency on acoustic agglomeration. L = 155 dB, t = 3 s. (a) Particle size distribution before and after acoustic agglomeration. (b) Evolution of total particle number concentration with time.

Effect of Particle Size Distribution

The effect of particle size distribution on the acoustic agglomeration is shown in Fig. 7. The initial particle size distributions can be approximately described using log-normal functions with the same geometric standard deviation but different geometric mean diameters (i.e., 0.15 μm, 0.3 μm and 0.5 μm). The acoustic frequency of 5000 Hz, the acoustic intensity of 155 dB and the residence time of 3 s are used in the simulations. It can be seen that the particle size distribution has a significant influence on the acoustic agglomeration. For initial distribution 1, most of the particles are fully entrained by the acoustic wave, only a small amount of relatively large particles exhibit different entrainment rates of oscillatory motion along with obvious drift-to-node motion. The motion behaviors of the relatively large particles lead to the orthokinetic interaction and the other acoustically induced interactions resulting from the entrainment motion of the particles. As the geometric mean diameter increases, for example, to 0.3 μm as represented by initial distribution 2, there are less particles that can be fully entrained and more particles with different entrainment rates. In this case, particles move with a greater relative velocity, which promotes the particle interaction and agglomeration. When the geometric mean diameter of the particles increases up to 0.5 μm as given by distribution 3, much more intense acoustic agglomeration occurs. Correspondingly, the peak of the particle size distribution decreases dramatically and the total particle number concentration decreases to 5% of its initial value in 1 s. The particle size distribution is an important factor affecting the acoustic agglomeration. Experimental investigations have demonstrated that with large additional particles as a second mode or with particle enlargement by heterogeneous condensation the removal of particles from the small particle range can be significantly enhanced (Hoffmann *et al.*, 1993; Wang *et al.*, 2011; Yan *et al.*, 2015).

CONCLUSIONS

The acoustic agglomeration process of $PM_{2.5}$ in the

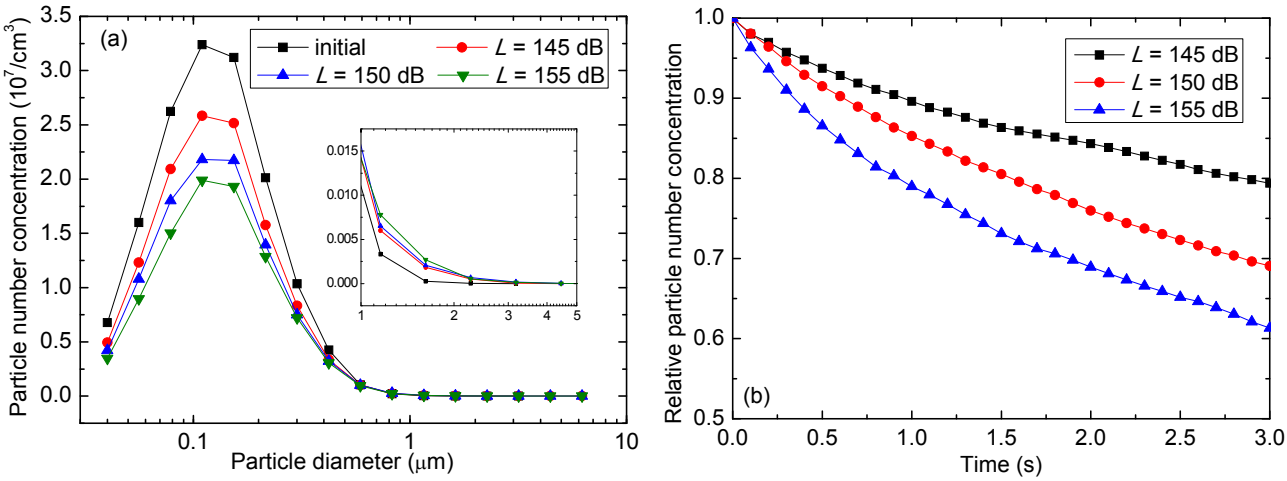

Fig. 6. Effect of acoustic intensity on acoustic agglomeration. f = 5000 Hz, t = 3 s. (a) Particle size distribution before and after acoustic agglomeration. (b) Evolution of total particle number concentration with time.

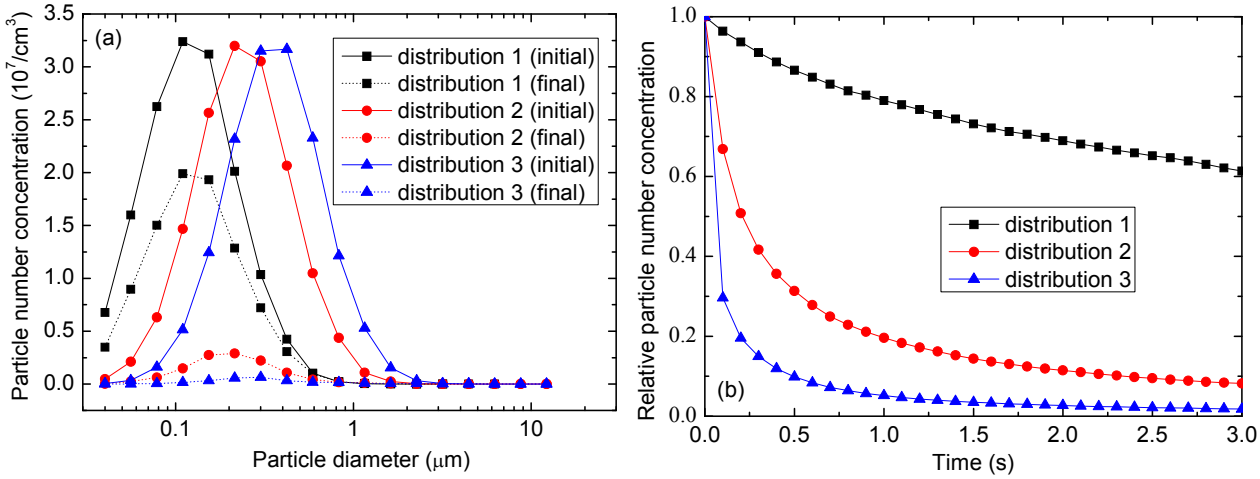

Fig. 7. Effect of particle size distribution on acoustic agglomeration. L = 155 dB, f = 5000 Hz, t = 3 s. (a) Particle size distribution before and after acoustic agglomeration. (b) Evolution of total particle number concentration with time.

standing wave has been modeled using the DSMC method. The effects of the drag force resulting in orthokinetic interaction and the gravitational force leading to gravity sedimentation on particle motion are taken into account, therefore the particle trajectories can be tracked. The contributions of other mechanisms such as the Brownian diffusion, the acoustic radiation pressure effect and the acoustic wake effect are included by a simple addition of the relevant collision rates to that obtained from the relative velocity based on the particle motion.

The simulation results are verified by the experimental data. On this basis the processes of acoustic agglomeration are studied by considering different acoustic mechanisms and varying key operating parameters, such as the residence time, the acoustic frequency, the acoustic intensity and the particle size distribution. The simulation results show that the combined effect of the orthokinetic interaction and the gravity sedimentation plays a dominant role in governing the acoustic agglomeration. The effect of the Brownian diffusion on the particle agglomeration is marginal. Compared with the mutual radiation pressure effect, the acoustic wake effect appears more influential on the acoustic agglomeration. The visualization of the acoustic agglomeration process reveals the critical feature of "orthokinetic drift" involved in the orthokinetic interaction and shows the high concentration regions resulting from the "orthokinetic drift". It is also found that the particle agglomeration phenomenon is more pronounced for higher acoustic frequency, higher acoustic intensity and larger particles. This work provides valuable data and vital information for the future optimization of acoustic agglomeration in the standing wave.

ACKNOWLEDGMENTS

This work is supported by the National Natural Science Foundation of China (51206113, 51176128 and 51576130) and Shanghai Science and Technology Commission, China (13DZ2260900). We gratefully acknowledge the computing time granted by the Computing Center at University of Shanghai for Science and Technology, China.

REFERENCES

Bruneau, M. (2006) *Fundamentals of Acoustics*. ISTE Ltd, London.

Capéran, P., Somers, J., Richter, K. and Fourcaudot, S. (1995). Acoustic agglomeration of a glycol fog aerosol influence of particle concentration and intensity of the sound field at two frequencies. *J. Aerosol Sci.* 26: 595–612.

Chang, Q., Zheng, C., Gao, X., Chiang, P., Fang, M., Luo, Z. and Cen, K. (2015). Systematic approach to optimization of submicron particle agglomeration using ionic-wind-assisted pre-charger. *Aerosol Air Qual. Res*. 15: 2709–2719.

Chen, H., Cao, J., Zhang, R. and Shen, X. (2008). Study on vibrating velocity in high-intensity standing wave field. *J. Southeast Univ.* 38: 75–80.

Chou, K.H. and Shaw, D.T. (1981). Acoustic agglomeration theory. In *Winter Annual Meeting of the Noise Control & Acoustics Division of the American Society of Mechanical Engineers*, *Washington, D. C., USA, 1981, the American* Society of Mechanical Engineers, New York, pp. 1–6.

Chou, K.H., Lee, P.S., Wegrzyn, J. and Shaw, D.T. (1982). Aerosol deposition in acoustically induced turbulent flow. *Atmos. Environ*. 16: 1513–1522.

Cleckler, J., Elghobashi, S. and Liu, F. (2012). On the motion of inertial particles by sound waves. *Phys. Fluids*. 24: 033301.

Czyz, H. (1987). The aerosol particle drift in a standing wave field. *Arch. Acoust.* 12: 199–214.

Czyz, H. (1990). On the concentration of aerosol particles by means of drift forces in a standing wave field. *Acustica* 70: 23–28.

De Sarabia, E.R.F., Elvira-Segura, L., González-Gómez, I., Rodríguez-Maroto, J.J., Muñoz-Bueno, R. and Dorronsoro-Areal, J.L. (2003). Investigation of the influence of humidity on the ultrasonic agglomeration of submicron particles in diesel exhausts. *Ultrasonics* 41: 277–281.

Dianov, D.B., Podolskii, A.A. and Turubarov V.I. (1968). Calculation of the hydrodynamic interaction of aerosol particles in a sound field under Oseen flow conditions. *Sov. Phys. Acoust.* 13: 367–374.

Dong, S., Lipkens, B. and Cameron, T.M. (2006). The effects of orthokinetic collision, acoustic wake, and gravity on acoustic agglomeration of polydisperse aerosols. *J. Aerosol Sci.* 37: 540–553.

Ehrlich, C., Noll, G., Kalkoff, W.D., Baumbach, G. and Dreiseidler, A. (2007). PM_{10}, $PM_{2.5}$ and $PM_{1.0}$—Emissions from industrial plants—Results from measurement programmes in Germany. *Atmos. Environ*. 41: 6236–6254.

Ezekoye, O.A. and Wibowo, Y.W. (1999). Simulation of acoustic agglomeration processes using a sectional algorithm. *J. Aerosol Sci.* 30: 1117–1138.

Fan, F. (2008). *Study on Growth Mechanisms of Inhalable Particles in Acoustic Field and in Supersaturated Vapor Environment*, Southeast University, Nanjing.

Fan, F., Yang, L., Yan, J., Bao, J. and Shen, X. (2009). Experimental investigation on removal of coal-fired fine particles by condensation scrubber. *Chem. Eng. Process*. 48: 1353–1360.

Fan, F., Yang, X. and Kim, C.N. (2013). Direct simulation of inhalable particle motion and collision in a standing wave field. *J. Mech. Sci. Technol*. 27: 1707–1712.

Friedlander, S.K. (1997). *Smoke, Dust and Haze: Fundamentals of Aerosol Behavior*, Wiley, New York.

Funcke, G. and Frohn, A. (1995). Comparison of Brownian and acoustic coagulation processes. Proceedings of 3rd European Symposium, Separation of particles from gases, Nurnberg, Germany, 1995, NurnbergMesse GmnH, Nurnberg, pp. 203–211.

Gallego-Juárez, J.A., De Sarabia, E.R.F., Rodríguez-Corral, G., Hoffmann, T.L. and Gálvez-Moraleda, J.C. (1999). Application of acoustic agglomeration to reduce fine particle emissions from coal combustion plants. *Environ. Sci. Technol.* 33: 3843–3849.

González, I., Hoffmann, T.L. and Gallego, J.A. (2000). Precise measurements of particle entrainment in a standing-wave acoustic field between 20 and 3500 Hz. *J. Aerosol Sci.* 31: 1461–1468.

González, I., Elvira, L., Hoffmann, T.L. and Gallego, J.A. (2001). Numerical study of the hydrodynamic interaction between aerosol particles due to the acoustic wake effect. *Acta Acust.* 87: 454–460.

González, I., Hoffmann, T.L. and Gallego, J.A. (2002). Visualization of hydrodynamic particle interactions: Validation of numerical model. *Acta Acust united Ac.* 88: 19–26.

González, I., Gallego, J.A and Riera, E. (2003). The influence of entrainment on acoustically induced interactions between aerosol particles—An experimental study. *J. Aerosol Sci.* 34: 1611–1631.

Hoffmann, T.L., Chen, W., Koopmann, G.H., Scaroni, A.W. and Song, L. (1993). Experimental and numerical analysis of bimodal acoustic agglomeration. *J. Vib. Acoust.* 115: 232–240.

Hoffmann, T.L. and Koopmann, G.H. (1996). Visualization of acoustic particle interaction and agglomeration: Theory and experiments. *J. Acoust. Soc. Am.* 99: 2130–2141.

Hoffmann, T.L. (1997). An extended kernel for acoustic agglomeration simulation based on the acoustic wake effect. *J. Aerosol Sci.* 28: 919–936.

Hoffmann, T.L. and Koopmann, G.H. (1997). Visualization of acoustic particle interaction and agglomeration: Theory evaluation. *J. Acoust. Soc. Am.* 101: 3421–3429.

Hoffmann, T.L. (2000). Environmental implications of acoustic aerosol agglomeration. *Ultrasonics* 38: 353–357.

Kashkoush, I. and Busnaina A. (1993). Submicron particle removal using ultrasonic cleaning. *Part. Sci. Technol*. 11: 11–24.

Komarov, S.V., Yamamoto, T., Uda, T. and Hirasawa, M. (2004). Acoustically controlled behavior of dust particles in high temperature gas atmosphere. *ISIJ Int.* 44: 275–284.

Li, X., Wang, Y., Guo, X. and Wang, Y. (2013). Seasonal variation and source apportionment of organic and inorganic compounds in $PM_{2.5}$ and PM_{10} particulates in Beijing, China. *J. Environ. Sci*. 25: 741–750.

Liu, J., Zhang, G., Zhou, J., Wang, J., Zhao, W. and Cen,

K. (2009). Experimental study of acoustic agglomeration of coal-fired fly ash particles at low frequencies. *Powder Technol*. 193: 20–25.

Liu, J., Wang, J., Zhang, G., Zhou, J. and Cen, K. (2011). Frequency comparative study of coal-fired fly ash acoustic agglomeration. *J. Environ. Sci.* 23: 1845–1851.

Manoucheri, M. and Ezekoye, O.A. (1996). Polystyrene soot agglomeration enhancement in an ultrasonic acoustic field. *Hazard. Waste Hazard. Mater.* 13: 121–130.

Pui, D.Y.H., Chen, S. and Zuo Z. (2014). $PM_{2.5}$ in China: Measurements, sources, visibility and health effects, and mitigation. *Particuology* 13: 1–26.

Rajendran, N., Wegrzyn, J., Cheng, M.T. and Shaw, D.T. (1979). Acoustic precipitation of aerosol under standing-wave condition. *J. Aerosol Sci.* 10: 329–338.

Sharifi, R., Miller, S.F., Scaroni, A.W., Koopmann, G.H. and Chen W. (1994). In situ monitoring of the acoustic agglomeration of fly ash particles. *ASME Cogen-Turbo* 9: 549–555.

Shaw, D.T. and Tu, K.W. (1979). Acoustic particle agglomeration due to hydrodynamic interaction between monodisperse aerosols. *J. Aerosol Sci.* 10: 317–328.

Sheng, C. and Shen, X. (2006). Modelling of acoustic agglomeration processes using the direct simulation Monte Carlo method. *J. Aerosol Sci.* 37: 16–36.

Sheng, C. and Shen, X. (2007). Simulation of acoustic agglomeration processes of poly-disperse solid particles. *Aerosol Sci. Technol.* 41: 1–13.

Song, L. (1990). *Modelling of Acoustic Agglomeration of Fine Aerosol Particles*. The Pennsylvania State University, University Park.

Song, X. and Fan, F. (2016). Analysis of the factors influencing the drift of inhalable particles in a standing wave acoustic field. *J. Eng. Thermal Energy Power* 35: 287–331.

Spengler, J. and Jekel, M. (2000). Ultrasound conditioning of suspensions—studies of streaming influence on particle aggregation on a lab- and pilot-plant scale. *Ultrasonics* 38: 624–628.

Tiwary, R., Reethof, G. and McDaniel, O.H. (1984). Acoustically generated turbulence and its effect on acoustic agglomeration. *J. Acoust. Soc. Am.* 76: 841–849.

Tsuji, Y., Tanaka, T. and Yonemura, S. (1998). Cluster patterns in circulating fluidized beds predicted by numerical simulation (discrete particle model versus two-fluid model). *Powder Technol.* 95: 254–264.

Volk, M.JR. and Moroz, W.J. (1976). Sonic agglomeration of aerosol particles. *Water Air Soil Pollut.* 5: 319–334.

Wang, J., Liu, J., Zhang, G., Zhou, J. and Cen, K. (2011). Orthogonal design process optimization and single factor analysis for bimodal acoustic agglomeration. *Powder Technol.* 210: 315–322.

Wei, J. (2013). A fast Monte Carlo method based on an acceptance-rejection scheme for particle coagulation. *Aerosol Air Qual. Res.* 13: 1273–1281.

Yan, J., Chen, L. and Yang, L. (2015). Combined effect of acoustic agglomeration and vapor condensation on fine particles removal. *Chem. Eng. J.* 290: 319–327.

Yang, L., Bao, J., Yan, J., Liu, J., Song, S. and Fan, F. (2010). Removal of fine particles in wet flue gas desulfurization system by heterogeneous condensation. *Chem. Eng. J.* 156: 25–32.

Yang, X. and Fan, F. (2015). Numerical simulation on motion of chain-like particle aggregates in standing wave acoustic field. *J. Chin. Soc. Power Eng*. 35: 287–291.

Zhang, G., Liu, J., Wang, J., Zhou, J. and Cen, K. (2011). Numerical simulation of acoustic agglomeration by quadrature method of moments. *CIESC J*. 62: 922–927.

Zhang, G., Liu, J., Wang, J., Zhou, J. and Cen, K. (2012). Numerical simulation of acoustic agglomeration by improved sectional algorithm. *J. Combust. Sci. Technol.* 18: 44–49.

Zhang, M. and Fan, F. (2012). Progress and prospect in numerical simulation on acoustic agglomeration of fine particles. *Chem. Ind. Eng. Prog.* 31: 1671–1676.

Zhao, B. (2007). *Study on the Removal of Inhalable Particles from Combustion by Acoustic agglomeration*, Southeast University, Nanjing.

Zhao, H., Zheng, C. and Xu, M. (2005). Multi-Monte Carlo method for particle coagulation: Description and validation. *Appl. Math. Comput.* 167: 1383–1399.

Received for review, August 10, 2016
Revised, February 6, 2017
Accepted, March 10, 2017